

Article

Not peer-reviewed version

# Identification and Characterization of a Novel Alginate Lyase from *Mesonia hitae* R32 Exhibiting High Thermal Stability and Potent Antioxidant Oligosaccharide Production

[Yongshang Ye](#), [Zhiyu Li](#), [Ying Zhou](#)<sup>\*</sup>, [Xiujun Gao](#)<sup>\*</sup>, Dingfan Yan

Posted Date: 17 March 2025

doi: 10.20944/preprints202503.1253.v1

Keywords: alginate lyase; alginate oligosaccharides; PL6 family; enzymatic properties; antioxidant activity



Preprints.org is a free multidisciplinary platform providing preprint service that is dedicated to making early versions of research outputs permanently available and citable. Preprints posted at Preprints.org appear in Web of Science, Crossref, Google Scholar, Scilit, Europe PMC.

Copyright: This open access article is published under a Creative Commons CC BY 4.0 license, which permit the free download, distribution, and reuse, provided that the author and preprint are cited in any reuse.

## Article

# Identification and Characterization of A Novel Alginate Lyase from *Mesonía hitae* R32 Exhibiting High Thermal Stability and Potent Antioxidant Oligosaccharide Production

Yongshang Ye, Zhiyu Li, Ying Zhou \*, Xiujun Gao \* and Dingfan Yan

Department of Biotechnology, School of Marine Science and Technology, Harbin Institute of Technology, Weihai, 264209, China

\* Correspondence: zhou.ying@hit.edu.cn (Y.Z.); gaoxiujun@hitwh.edu.cn (X.J.G.)

**Abstract:** Alginate lyases are of great importance in biotechnological and industrial processes, yet research on these enzymes from *Mesonía* genus bacteria is still limited. In this study, a novel PL6 family alginate lyase, MhAly6, was cloned and characterized from the deep-sea bacterium *Mesonía hitae* R32. The enzyme, composed of 797 amino acids, contains both PL6 and GH28 catalytic domains. Phylogenetic analysis revealed its classification into the subfamily 1 of the PL6 family. MhAly6 showed optimal activity at 45°C and pH 9.0, retaining over 50% activity after 210 min of incubation at 40°C, highlighting its remarkable thermal stability. The enzyme exhibited degradation activity toward sodium alginate, poly M, and poly G, with the highest affinity for its natural substrate, sodium alginate, producing alginate oligosaccharides (AOS) with degrees of polymerization (DP) ranging from 2 to 7. Molecular docking identified conserved catalytic sites (Lys241/Arg262) and calcium-binding sites (Asn202/Glu234/Glu236), while the GH28 domain played an auxiliary role in substrate binding. Antioxidant assays revealed that MhAly6-derived AOS showed potent radical-scavenging activity, achieving 80.64% and 95.39% inhibition rates against DPPH and ABTS radicals, respectively, highlighting their potential as natural antioxidants. This work provides a promising candidate for developing efficient alginate lyases and functional AOS, while expanding the application potential of *Mesonía* genus bacteria.

**Keywords:** Alginate lyase; Alginate oligosaccharides; PL6 family; Enzymatic properties; Antioxidant activity

## 1. Introduction

Alginic acid is an acidic linear polysaccharide composed of  $\beta$ -D-mannuronic acid (M) and  $\alpha$ -L-guluronic acid (G), linked by  $\beta$ -1,4-glycosidic bonds. It is widely found in the cell walls and intracellular matrices of brown algae (e.g., *Laminaria*, *Macrocystis*) [1]. Based on the composition of sugar units, alginic acid can be classified into poly  $\beta$ -D-mannuronic acid (poly M), poly  $\alpha$ -L-guluronic acid (poly G), or heteropolymers. Sodium alginate, as a hydrocolloid, has broad applications in biomedicine [2], wastewater purification [3], and soil improvement [4,5]. However, its poor solubility and bioavailability limit its utilization. Alginate oligosaccharides (AOS), small-molecule products derived from the hydrolysis of alginate with degrees of polymerization (DP) typically ranging from 2 to 25 [1], exhibit superior solubility and broader application potential due to their lower molecular weight (Mw). Recently, AOS have attracted significant attention for their diverse biological functions, including antioxidant [6], antitumor [7], immunomodulatory [8,9], and plant growth-regulating activities [10,11], highlighting their value in biomedical research [12,13] and agriculture [14,15].

The  $\beta$ -1,4-glycosidic bonds in sodium alginate can be cleaved via physical, chemical, or enzymatic methods to produce AOS. Physical [15,16] and chemical approaches [17] face challenges

such as high equipment costs, operational risks, and byproduct pollution. In contrast, enzymatic hydrolysis offers advantages of high efficiency, mild condition, and low energy consumption [18,19]. During enzymatic degradation, alginate lyases catalyze  $\beta$ -elimination reactions to break  $\beta$ -1,4-glycosidic bonds, generating monosaccharides or oligosaccharides. Based on substrate specificity, alginate lyases are categorized into three groups: poly M lyases (EC 4.2.2.3), poly G lyases (EC 4.2.2.11), and bifunctional enzymes capable of degrading both poly M and poly G. According to the CAZy database, alginate lyases are classified into 16 polysaccharide lyase (PL) families (PL5, 6, 7, 8, 14, 15, 17, 18, 31, 32, 34, 36, 38, 39, 41, and 44) based on the sequence homology of the catalytic domain [20]. Endolytic alginate lyases randomly cleave internal glycosidic bonds to produce low-DP unsaturated AOS, while exolytic enzymes generate unsaturated monosaccharides. Currently characterized alginate lyases are primarily derived from marine microorganisms, such as *Vibrio* [21,22], *Microbulbifer* [23], *Flavobacterium* [24], and *Streptomyces* [25,26]. The genus *Mesonina*, first reported by Nedashkovskaya *et al.* in 2003 [27], comprises 11 validly published species (<https://lpsn.dsmz.de/genus/mesonina>, accessed on February 26, 2025) [28]. However, research on *Mesonina* remains largely focused on novel species identification, with limited studies on functional proteins. Numerous genes in sequenced *Mesonina* genomes remain uncharacterized [29].

In our previous work, the bacterial strain *Mesonina hitae* R32 was isolated from a depth of 150 m in the South Atlantic Ocean (13.36°W, 15.17°S), demonstrating growth capability with sodium alginate as the sole carbon source. However, the enzymatic properties and degradation mechanisms of its alginate lyase remain unelucidated [30]. In this study, a novel PL6 family alginate lyase, MhAly6, from the *Mesonina hitae* R32 was cloned and expressed. The enzyme exhibited excellent thermal stability and tolerance to metal ions, effectively degrading sodium alginate to produce AOS with a DP ranging from 2 to 7. These AOS showed significant antioxidant activity.

## 2. Results and Discussion

### 2.1. Analysis of Gene and Protein Sequence of MhAly6

The open reading frame of the *MhAly6* gene spans 2391 bp, encoding a protein consisting of 797 amino acid residues. The predicted structure of MhAly6 includes an N-terminal signal peptide (Met1-Ser23, 23 amino acids), a PL6 family domain (Val28-Ala393), and a GH28 family domain (Pro550-Ile696) (Figure 1a). Notably, MhAly6 is distinguished from previously reported alginate lyases by the presence of a GH28 family domain. According to the CAZy database, proteins in the GH28 family are predominantly polygalacturonases (pectinases) [31], however, no pectin-degrading activity was detected for MhAly6 in this study (data not shown). The theoretical Mw of mature MhAly6 is approximately 86.70 kDa, with an isoelectric point of 7.58 and an instability index (II) of 28.26, indicating that it can be classified as a stable protein. Predictions from the SoluProt server suggested that MhAly6 could be expressed in soluble form in *Escherichia coli*, which was experimentally validated in subsequent studies. NCBI sequence alignment revealed that MhAly6 shares the highest similarity (84.65%) with an uncharacterized PL6 family protein from *Salegentibacter echinorum* (WP083572075). Phylogenetic analysis placed MhAly6 within subfamily 1 of the PL6 family (Figure 1b). Its sequence similarities to characterized enzymes were as follows: 56.34% with Celly0294 from *Cellulophaga lytica* DSM 7489 [32], 53.23% with AlyGC from *Glaciecola chathamensis* S18K6<sup>T</sup> [33], 50.41% with BcAlyPL6 from *Bacteroides clarus* YIT 12056 [34], 40.26% with Rmar1165 from *Rhodothermus marinus* DSM 4252 [32], and 40.26% with AlyRm6A from *Rhodothermus marinus* 4252 [35]. Combined conserved domain analysis and multiple sequence alignment identified Lys241 and Arg262 as the Brønsted base and acid, respectively, participating in the catalysis. Additionally, Asn202, Glu234, and Glu236 were proposed as calcium-binding sites. These residues were subsequently validated by molecular docking and are highly conserved in the characterized alginate lyases of PL6 family (Figure 1c). Overall, MhAly6 has been identified as a novel dual domain alginate lyase of the PL6 family.

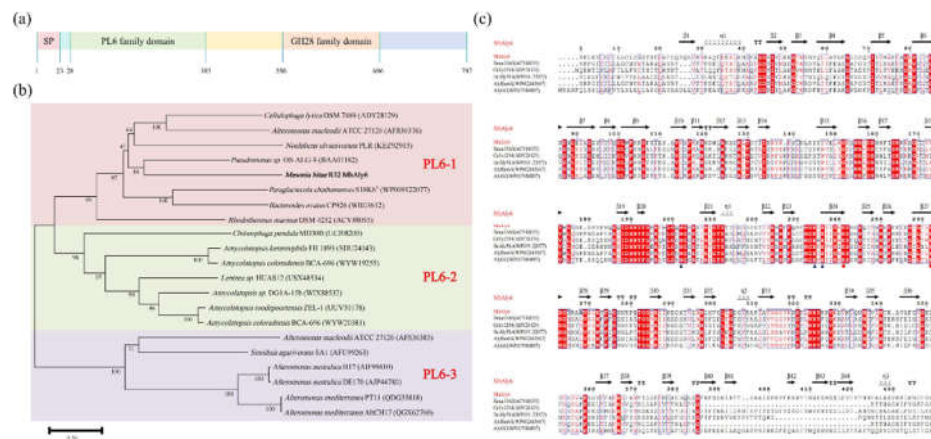


**Figure 1.** Comprehensive characterization of MhAly6 using multiple tools. (a) Conserved domain analysis. (b) Phylogenetic analysis of MhAly6 and other alginate lyases of the PL6 family. Subfamilies 1, 2, and 3 are highlighted with pink, green, and purple shading, respectively, and their names are labeled in red text. (c) Multiple sequence alignment analysis of MhAly6 with selected alginate lyases of the PL6 family (partial sequences). Catalytic sites and Ca<sup>2+</sup> binding sites are marked with red circles and blue triangles, respectively.

2.2. Biochemical Characterization of MhAly6

The full-length MhAly6 gene was successfully cloned and expressed in *E. coli* BL21(DE3). Purification results revealed a single clear band between 66.2 kDa and 116.0 kDa, consistent with the theoretical Mw of the MhAly6 (86.70 kDa) (Figure 2a).

MhAly6 exhibited maximum activity at its optimal temperature of 45°C, retaining over 80% activity at 35°C, 50°C, and 55°C (Figure 2b). After incubation for 60 min at 40°C, approximately 80% activity remained, and over 50% activity was retained even after 210 min. However, the activity decreased to 60% and 10% after incubation at 45°C and 50°C after 60 min, with 90% and 100% loss observed after 210 min, respectively (Figure 2c). As shown in Table 1, most reported alginate lyases of the PL6 family exhibit optimal temperatures between 30°C–45°C. For instance, TsAly6A, ALFA4, AlyM2, AlgL6, AlyRm1, and TAPL6 show maximum activity below 40°C, while AlyPL6 shares the same optimal temperature (45°C) as MhAly6. VpAly-VII and AlyRmA exhibit even higher optimal temperatures (>45°C). Notably, MhAly6 demonstrated superior thermal stability compared to most enzymes, retaining more than 50% activity after incubation at 40°C for 210 min, whereas others lost more than 50% activity within 60 min under similar conditions. Previous studies suggested that the proportion of proline and arginine residues correlates with thermal stability. The rigid cyclic side chain of proline restricts the backbone conformational flexibility [36], while the highly protonated guanidinium group of arginine facilitates diverse electrostatic interactions at physiological pH [37]. AlyRmA, with the highest reported thermal stability among the PL6 family enzymes listed in Table 1, contains 6.88% proline and 9.12% arginine. In contrast, MhAly6 has only 3.39% and 2.26% of these residues. This implies that enhancing proline/arginine content via amino acid substitution could further improve the thermal stability of MhAly6. As for optimal pH, MhAly6 activity increased under alkaline conditions, with peak activity observed at pH 9.0, and retaining 86.19% residual activity at pH 10.0 (Figure 2d). Considering that alkaline pretreatment is commonly employed in the extraction of alginate from brown algae, the alkaliphilic properties of the MhAly6 are well-suited for industrial applications.

Consistent with most alginate lyases, MhAly6 displayed Na<sup>+</sup>-dependent activation (Figure 2e). The enzyme activity increased with Na<sup>+</sup> concentration, reaching 3.14-fold of the control at 200 mM. Even at Na<sup>+</sup> concentrations ranging from 300 to 900 mM, the activity remained over twice the control level. Substrate specificity assays revealed that MhAly6 had relative activities of 100%, 15.20%, and 20.28% for sodium alginate, poly M, and poly G, respectively (Figure 2f). This indicated a strong preference for natural sodium alginate over homopolymeric substrates.



The effects of various metal ions and chemicals on MhAly6 were also investigated (Figure 2g). The enzyme activity was enhanced by  $\text{Ca}^{2+}$ ,  $\text{Mg}^{2+}$ , and glycine at all tested concentrations (1-10 mM or 0.1-1%). In contrast,  $\text{Mn}^{2+}$ , EDTA, and SDS strongly inhibited the activity at low concentrations (1 mM/0.1%). Specifically, EDTA binds to the divalent metal ions in MhAly6 (e.g.,  $\text{Ca}^{2+}$ ), forming stable chelates that remove the metal ions from the enzyme, ultimately leading to its deactivation. SDS could disrupt the hydrophobic interactions critical for maintaining the tertiary structure of the enzyme. This made the enzyme lose its native conformation, and the spatial structure of the active site was disrupted, preventing substrate binding or catalysis. At higher concentrations (5-10 mM/0.5-1%), most of the tested metal ions and chemical reagents reduced the enzyme activity. However,  $\text{Ni}^{2+}$  showed a unique trend. It inhibited the activity at a low concentration (1 mM), enhanced the activity at a moderate concentration (5 mM), and then -inhibited it again at a high concentration (10 mM). In industrial processes for preparing AOS from brown algae, various metal ions are inevitably introduced. MhAly6's tolerance to common industrial metal ions highlights its significant practical potential.

In summary, although MhAly6 did not surpass all reported enzymes of the PL6 family in every aspect, its exceptional thermal stability, tolerance to metal ions, and strong affinity for natural alginate make it a highly promising candidate for degrading complex brown algal biomass.

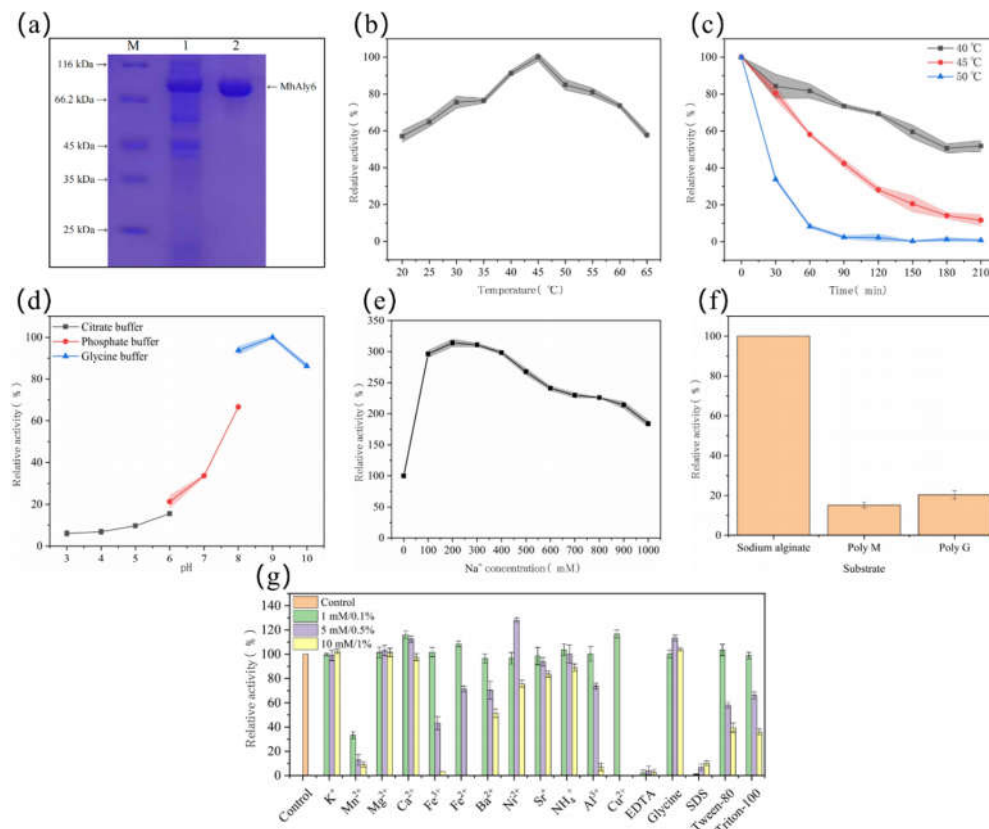


**Figure 2.** Biochemical characterization of the MhAly6. (a) SDS-PAGE analysis of the purified MhAly6. (b) Relative activity of the MhAly6 at different temperatures (20-65°C). (c) Thermal stability of the MhAly6 at various temperatures (40-50°C). (d) Relative activity of the MhAly6 at different pH values (3-10). (e) Relative activity of the MhAly6 at varying  $\text{Na}^+$  concentrations (0-1000 mM). (f) Substrate specificity of the MhAly6 toward sodium alginate, Poly M, and Poly G. (g) Effects of metal ions and chemical reagents on the activity of MhAly6.

**Table 1.** Characteristics of the PL6 family alginate lyases from different sources: a recent overview.

Enzyme	Source	Substrate Specificity <sup>a</sup>	AOS products (DP)	Action Mode	Activators <sup>b</sup>	Inhibitors <sup>c</sup>	Optimal Temperature (°C)/pH	Stability	Reference
MhAly6	<i>Mesonia hitae</i> R32	SA>PM>PG	2-7	Exo	Ni <sup>2+</sup> (5 mM); Cu <sup>2+</sup> (1 mM); Ca <sup>2+</sup> (1 mM)	Cu <sup>2+</sup> (5 mM); EDTA(10 mM); Fe <sup>3+</sup> (10 mM)	45/9.0	40°C, 60 min, remaining 80%	This study
TsAly6A	<i>Thalassomonas</i> sp. LD5	PG>SA>PM	2-3	Endo	Ca <sup>2+</sup> (-); Mg <sup>2+</sup> (-); Fe <sup>3+</sup> (-)	EDTA(-); SDS(-); Na <sup>+</sup> (500 mM)	35/8.0	40 °C, 60 min, remaining 29%	[38]
ALFA4	<i>Formosa algae</i> KMM 3553 <sup>r</sup>	-	2(Main)	-	-	-	30/8.0	37 °C, 100 min, remaining 50%	[39]
AlyPL6	<i>Pedobacter hainanensis</i> NJ-02	SA>PG>PM	2-6	Exo	Na <sup>+</sup> (1 mM)	Mn <sup>2+</sup> (1 mM); Zn <sup>2+</sup> (1 mM); Co <sup>2+</sup> (1 mM)	45/10	40 °C, 60 min, remaining 50%	[40]
OUC-ScCD6	<i>Streptomyces colicolor</i> A3(2)	SA>PM>PG	2-10	Endo	Mn <sup>2+</sup> (1 mM); Fe <sup>3+</sup> (1 mM); Zn <sup>2+</sup> (1 mM)	EDTA(1 mM); Ni <sup>2+</sup> (1 mM); Cu <sup>2+</sup> (1 mM)	50/9.0	40 °C, 60 min, remaining 50%	[41]
AlyM2	<i>Pseudoalteromonas arctica</i> M9	PMG>SA>PM>PG	3(Main)	-	-	-	30/8.0	-	[42]
AlgL6	<i>Microbulbifer</i> sp. ALW1	PG>SA>PM	2-4	Exo	Tween 80(1%); Tween 20(1%); Na <sup>+</sup> (500 mM)	Cu <sup>2+</sup> (10 mM); Fe <sup>2+</sup> (10 mM); Ba <sup>2+</sup> (10 mM)	35/8.0	40 °C, 60 min, remaining 19%	[43]
VpAly-VII	<i>Vibrio pelagius</i> WXL662	SA>PM>PG	3-6	Endo	-	-	50/8.0	-	[44]
AlyRm1	<i>Rubrivirga marina</i>	PM>SA>PG	2-5	Exo	SDS(1 mM); Ca <sup>2+</sup> (1 mM); K <sup>+</sup> (1 mM)	EDTA(1 mM); Zn <sup>2+</sup> (1 mM); Mn <sup>2+</sup> (1 mM)	30/10.0	40 °C, 60 min, remaining 20%	[45]
TAPL6	<i>Thalassotaleaalgicola</i>	PM>SA>PG	2-6	Exo	Mg <sup>2+</sup> (1 mM); Ca <sup>2+</sup> (1 mM); K <sup>+</sup> (1 mM)	Zn <sup>2+</sup> (1 mM); Fe <sup>2+</sup> (1 mM); Ni <sup>2+</sup> (1 mM)	25/10.0	40 °C, 60 min, remaining 20%	[46]
AlyRmA	<i>Rhodothermus marinus</i>	SA>PM>PG	2-4	Exo	Mg <sup>2+</sup> (1 mM); Ca <sup>2+</sup> (1 mM)	Cu <sup>2+</sup> (1 mM); Zn <sup>2+</sup> (1 mM); Ni <sup>2+</sup> (1 mM)	70/8.0	70 °C, 60 min, remaining 100%	[11]

a: SA: Sodium alginate; PM: poly M; PG: poly G; PMG: poly MG; -: Not determined; b: Those metal ions or chemical reagents that increased the enzyme activity under a certain concentration (the concentration); c: Those metal ions or chemical reagents that suppressed the enzyme activity under a certain concentration (the concentration).

2.3. Analysis of the Degradation Products of MhAly6

The degradation products of MhAly6 acting on three substrates (sodium alginate, poly M, and poly G) at different time points were analyzed using Thin-layer chromatography (TLC). The results (Figure 3a, b) revealed similar product profiles for sodium alginate and poly M, with

monosaccharides detected within 30 min of degradation. In contrast, monosaccharides from poly G degradation appeared only after 2 h (Figure 3c). Overall, MhAly6 generated identical types of products from all three substrates.

After 24 h of reaction, the final products of sodium alginate degradation by MhAly6 were analyzed via electrospray ionization mass spectrometry (ESI-MS) (Figure 3d). Signals at  $m/z$  193.03, 351.06, 527.09, and 703.12 corresponded to saturated monosaccharides, unsaturated disaccharides (DP 2), trisaccharides (DP 3), and tetrasaccharides (DP 4), respectively. Peaks at  $m/z$  923.12 and 1056.19 represented oligosaccharides with DP 5-7, including one or two  $\text{Na}^+$  adducts. As listed in Table 1, similar to other alginate lyases of the PL6 family, MhAly6 degraded sodium alginate in an exolytic mode, producing AOS with DP 2-7. Notably, MhAly6 is among the few alginate lyases capable of generating DP 7 oligosaccharides. These results highlight its strong potential for efficient sodium alginate degradation.

However, the heterogeneous mixture of high-DP products remains a significant challenge in AOS production using alginate lyases. In future studies, we plan to engineer MhAly6 through rational design and enzyme fusion technologies to enable the production of specific or single-DP AOS, thereby reducing downstream separation and purification costs.

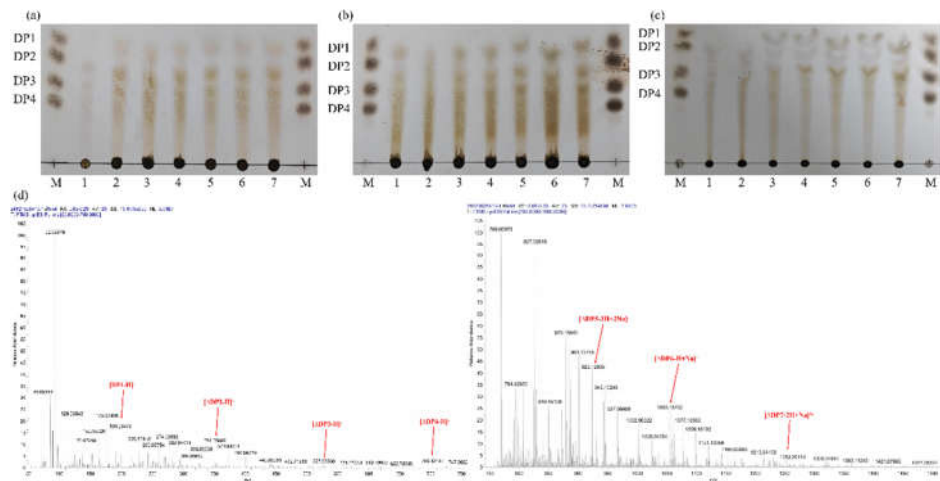


**Figure 3.** Analysis of the degradation products of MhAly6. (a-c) TLC analysis of the degradation products from sodium alginate, poly M, and poly G, respectively. M: DP 1-4 standards; Lanes 1-7: Degradation products of the three substrates at reaction times of 0.5 h, 1 h, 2 h, 3 h, 6 h, 12 h, and 24 h using purified MhAly6. (d) ESI-MS analysis of the sodium alginate degradation products after 24 h.

2.4. Structural Modeling and Evaluation of MhAly6

To predict the three-dimensional structure of MhAly6 with high precision, homology modeling using the SWISS-MODEL server and AlphaFold 3 were performed simultaneously. For the homology model of MhAly6 generated by SWISS-MODEL (Figure 4a), the Global Model Quality Estimation (GMQE) and Qualitative Model Energy Analysis (QMEAN) scores provided by the server were used for evaluation. According to previous studies, models are considered valid when GMQE and QMEAN scores fall within the ranges of 0-1 [47] and -4-0 [48], respectively. In this study, the homology model achieved GMQE and QMEAN values of 0.65 and -1.91, both meeting the criteria for validity. AlphaFold 3, a third-generation protein structure prediction model developed by DeepMind, represents a milestone in structural biology [49]. Benefiting from its advantages, we also employed AlphaFold 3 for modeling (Figure 4b). The results showed that the model predicted by AlphaFold 3 not only included the PL6 and GH28 family domains but also successfully captured the region of signal peptide, which was absent in the homology model.

The accuracy of both structures was further assessed using Ramachandran plot analysis via SAVES v6.0 (Figure 4c, d). According to the evaluation standards, models with more than 90% of

residues in the most favored regions are considered high-quality, while those with more than 80% are regarded as reliable [50]. The homology model had 82.70% of residues in the most favored regions, while the AlphaFold 3-predicted model showed 86.80%. Therefore, both models in this study were reliable. Notably, in the homology modeling, three residues were located in the disallowed regions, whereas the AlphaFold 3 model exhibited none. This clearly indicates the superior accuracy of the AlphaFold 3-predicted model. Although both models are valuable for future research, the structurally more complete AlphaFold 3-predicted model was selected for subsequent molecular docking studies between MhAly6 and DP 6 AOS.

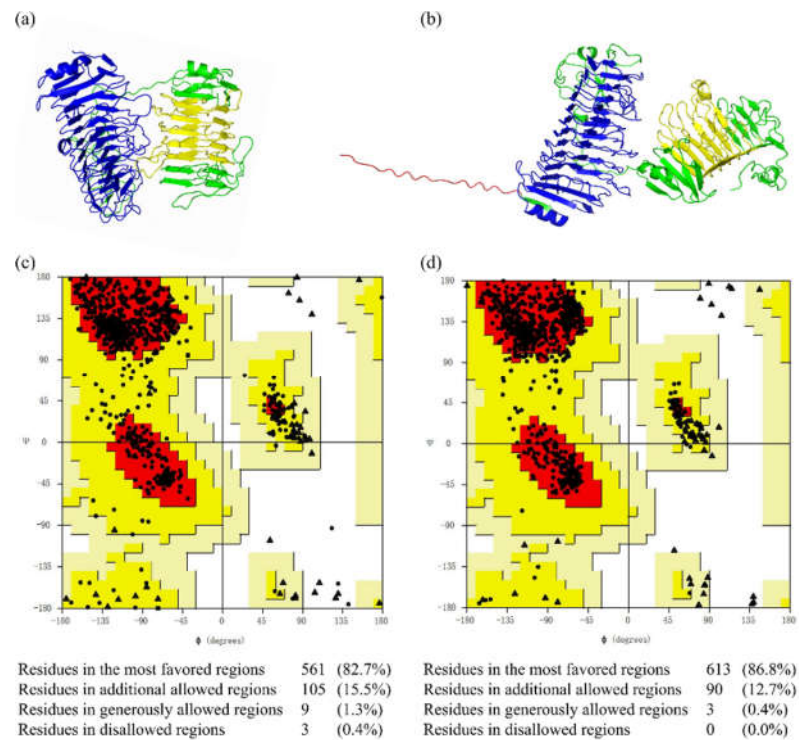


**Figure 4.** Structural modeling and evaluation of MhAly6. (a) Homology model generated by SWISS-MODEL. (b) The AlphaFold 3-predicted model. The signal peptide fragment is depicted in red, the PL6 family domain in blue, the GH28 family domain in yellow, and the remaining structure in green. (c) Ramachandran plot analysis of the homology model. (d) Ramachandran plot analysis of the AlphaFold 3-based model.

In order to identify the key substrate recognition sites of MhAly6, this study screened the molecular docking results with the lowest binding free energy for analysis. The results indicated that M6, G6, and H6 could bind to the cleft of the PL6 family domain of MhAly6 (Figure 5a-c), and this region was highly conserved (Figure 5d). Interestingly, although the substrate binding sites of M6, G6, and H6 were not exactly the same, the binding sites of G6 and H6 showed considerable similarity. Further examination of the binding interactions between the three substrates and MhAly6 revealed that in the MhAly6-M6 complex, Asn202, Glu205, Arg208, Ser212, Glu236, Lys241, Arg262, His263, Arg286, Arg308, Tyr325, Glu525, and Asn559 could form hydrogen bonds with the M6 molecule (Figure 5e). In the MhAly6-G6 complex, Asn202, Ser212, Glu236, Arg262, Lys241, His263, Glu281, Arg286, Asp305, Arg308, Glu525, Asn557, Asn559, and Ser590 could form hydrogen bonds with the G6 molecule (Figure 5f). In the MhAly6-H6 complex, Asn202, Glu205, Ser212, Glu234, Glu236, Lys241, Arg262, His263, Glu281, Arg286, Asp305, Arg308, Glu525, Asn557, Asn559, and Ser590 could form hydrogen bonds with the H6 molecule (Figure 5g). It is worth noting that ten residues-Asn202, Ser212, Glu236, Lys241, Arg262, His263, Arg286, Arg308, Glu525, and Asn559- could form hydrogen bonds with all three substrates in MhAly6 (Figure 5h). Except for Arg308, Glu525, and Asn559, the other seven residues were highly conserved (Figure 1c). Specifically, Asn202 and Glu236 served as



the binding sites for  $\text{Ca}^{2+}$ , while Lys241 and Arg262 were identified as the key catalytic residues. Interestingly, Glu525 and Asn559 were located in the GH28 family domain, which means that in MhAly6, the GH28 family domain played a complementary role in substrate binding. In *Zheng et al.*'s study, a similar phenomenon was observed. The alginate lyase AlyRm1 from *Rubrivirga marina*, which they characterized, contains a PL6 domain (Val24–Gly396) and a FlgD-Ig-like domain (Phe501–Ala562). In this enzyme, Glu543 located within the FlgD-Ig-like domain forms hydrogen bonds with G4 molecules, facilitating substrate binding [45]. This suggests that non-catalytic domains (such as other polysaccharide catalytic domains, carbohydrate-binding modules, or other unverified functional structures) have an undeniable effect on substrate binding by the catalytic domains in mature alginate lyases. This finding also reminds us the importance of considering the effects of non-catalytic domains when conducting truncation studies on high-molecular-weight alginate lyases, as these domains may significantly affect the enzyme function.

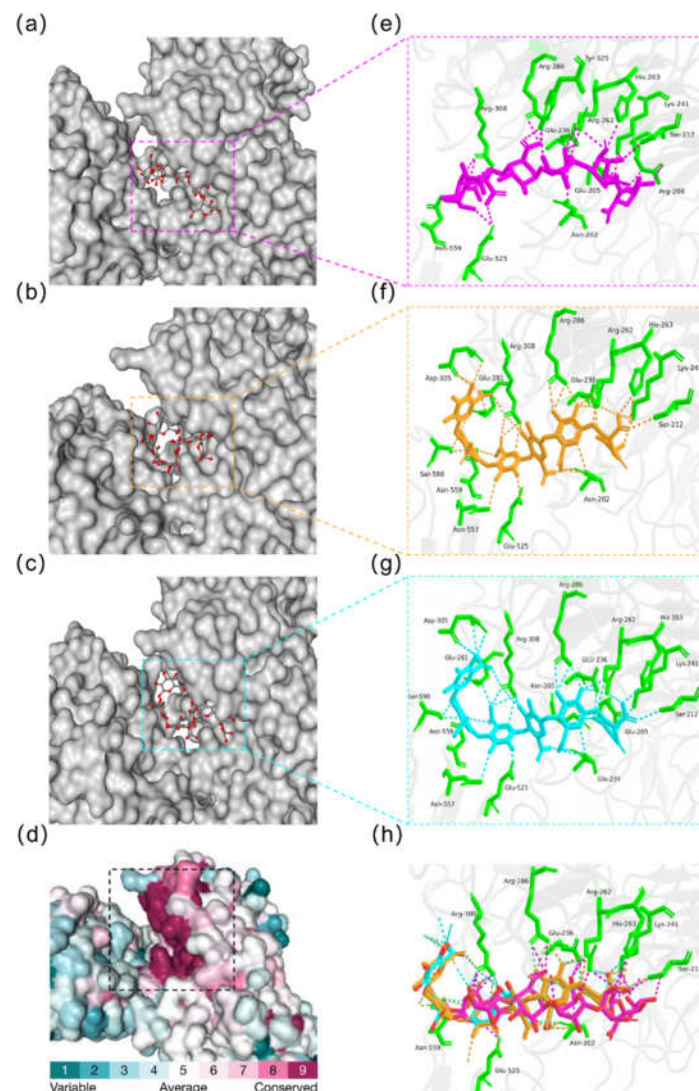


**Figure 5.** Substrate-binding groove, conservation analysis, and molecular docking results of MhAly6. (a-c) Binding positions of M6, G6, and H6 in MhAly6, respectively. (d) Evolutionary conservation analysis of MhAly6. Amino acid residues were analyzed using the ConSurf program, with conservation grades color-coded on a gradient from most variable (turquoise) to most conserved (maroon). (e-g) Key residues interacting with M6, G6, and H6 in MhAly6, respectively. Key residues are shown in green; M6, G6, and H6 molecules are depicted in purple, yellow, and blue, respectively. (h) Residues in MhAly6 interacting with all three substrates (M6, G6, and H6), using the same color scheme as above.

### 2.5. Antioxidant Activity of AOS Derived from MhAly6-Mediated Degradation

AOS derived from alginate degradation have attracted significant attention due to their exceptional antioxidant properties, with applications in food industries and pharmaceutical development. In this study, the antioxidant activity of AOS generated by MhAly6-mediated sodium alginate degradation was assessed using multiple assays, including ferric reducing power and the scavenging of hydroxyl, DPPH, and ABTS radicals.

Antioxidant activity is closely linked to reducing capacity, making ferric reducing power a common metric for assessing antioxidants. As shown in Figure 6a, the reducing power of AOS at 690 nm increased from 0.37 to 1.22 in a concentration-dependent manner. Reductones are a class of carbonyl-containing organic compounds with strong reducing properties. Their structural characteristics enable them to neutralize free radicals by donating hydrogen atoms, thereby interrupting oxidative chain reactions. The presence of reductone groups in AOS molecules confers electron-donating characteristics, allowing them to reduce high-valent metal ions (e.g.,  $\text{Fe}^{3+} \rightarrow \text{Fe}^{2+}$ ) while scavenging radicals.

The hydroxyl radical is a highly reactive oxygen species with potent oxidizing capacity. In biological systems, hydroxyl radical can attack deoxyribose and bases in DNA, leading to base modifications and strand breaks, ultimately resulting in gene mutations or apoptosis. As shown in Figure 6B, although the hydroxyl radical scavenging efficacy of AOS was less potent than ascorbic acid (Vc), its activity increased progressively with concentration. At 20 mg/mL, AOS achieved a hydroxyl radical scavenging rate of  $51.41 \pm 1.68\%$  (Figure 6b). Figure 6C shows that the same concentration (20 mg/mL) of AOS exhibited superior DPPH radical scavenging activity ( $80.64 \pm 1.40\%$ ), surpassing the results reported previously [51]. Remarkably, in Figure 6D, AOS at 3 mg/mL displayed an extraordinary ABTS radical scavenging rate of  $95.39 \pm 4.10\%$ , a phenomenon not observed in hydroxyl radical or DPPH radical scavenging experiments. According to Kelishomi *et al.*, the antioxidant mechanism of AOS may involve hydrogen atom transfer and radical adduct formation, with the formation of double bonds between C-4 and C-5 playing a crucial role in these interactions [52].

These findings collectively indicated that AOS derived from MhAly6-mediated alginate degradation possesses significant potential as a natural antioxidant for applications in food preservation, cosmetics, and nutraceuticals.

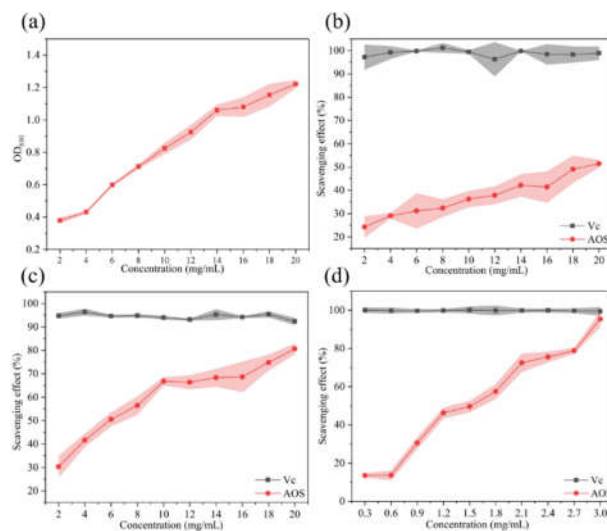


**Figure 6.** Antioxidant functions of AOS produced by MhAly6. (A) The ferric reducing ability of AOS. (B) Hydroxyl radical scavenging activity of AOS. (C) DPPH radical scavenging activity of AOS. (D) ABTS radical scavenging activity of AOS.

### 3. Materials and Methods

#### 3.1. Chemicals and Strains

Sodium alginate (viscosity:  $200 \pm 20$  mPa·s, purity  $\geq 98\%$ ) was purchased from Aladdin Biochemical Technology Co., Ltd. (Shanghai, China). Poly M (M content: 92.6%, G content: 7.4%) and Poly G (G content: 86.2%, M content: 13.8%) were obtained from Qingdao BZ Oligo Biotech Co., Ltd. (Qingdao, China). Kanamycin and isopro-pyl- $\beta$ -D-thiogalactopyranoside (IPTG) were acquired from Solarbio Science & Technology Co., Ltd. (Beijing, China). Other chemicals used in this study were of analytical grade. TLC silica gel plates (60F 254) were purchased from Merck Group (Darmstadt, Germany). Primers for MhAly6 gene cloning were synthesized by Sangon Biotech Co., Ltd. (Shanghai, China). *E. coli* DH5 $\alpha$  was used for plasmid construction, and *E. coli* BL21(DE3) was employed for protein expression.

#### 3.2. Bioinformatics Analysis

The genome of *Mesonnia hitae* R32 strain (GenBank ID: GCA008692195) was annotated for alginate lyases using the dbCAN2 database (<https://bcbl.unl.edu/dbCAN2/blast.php>). The signal peptide of MhAly6 was predicted using the SignalP 5.0 online tool (<https://services.healthtech.dtu.dk/services/SignalP-5.0/>). The protein domains of MhAly6 were analyzed via the NCBI Conserved Domain Database (<https://www.ncbi.nlm.nih.gov/Structure/cdd/wrpsb.cgi>). A phylogenetic tree of the PL6 subfamily alginate lyases was constructed using MEGA 11.0 software, based on the maximum likelihood method with 1000 bootstrap replicates. The multiple sequence alignment results were visualized using ESPript 3.0 (<http://esprict.ibcp.fr/ESPript/ESPript/>). The Mw, isoelectric point, and amino acid composition of MhAly6 were analyzed using the Expasy-ProtParam tool (<https://web.expasy.org/protparam/>). The solubility expression potential of this enzyme in *E. coli* was predicted using SoluProt (<https://loschmidt.chemi.muni.cz/soluprot/>).

#### 3.3. Cloning, Expression and Purification of MhAly6

The MhAly6 gene was amplified from the genomic DNA of *Mesonnia hitae* R32 using the forward primer (MhAly6-F: 5'-GGATCTTCCAGAGATTCTAGAATGCAAAAACAACTGGTGGAGAA-3' and the reverse primer (MhAly6-R: 5'-CTGCCGTTTCGACGATAAGCTTTTAATAACTTAATAGTCCTATGGTTTCTATACC-3'). The amplified fragment was then digested with *Xho*I and *Hind*III restriction enzymes and ligated into the pET28a(+) vector between the *Xho*I and *Hind*III restriction sites. The ligation product was subsequently transformed into *E. coli* DH5 $\alpha$  competent cells. The construct was sequenced by CWBIO Biotechnology Co., Ltd. (Taizhou, China) for verification. After confirmation, the plasmid was transformed into *E. coli* BL21(DE3) competent cells.

The alginate lyase MhAly6 was expressed in *E. coli* BL21(DE3). Briefly, the recombinant *E. coli* BL21(DE3) strain harboring the MhAly6 gene was inoculated at (2% v/v) into LB broth containing kanamycin (100 mg/L) and cultured at 37°C with shaking at 150 rpm until the OD<sub>600</sub> reached approximately 0.5. Protein expression was induced by adding IPTG to a final concentration of 0.1 mM. Following induction, the culture was incubated at 16°C with shaking at 150 rpm for 16 h to produce large quantities of the recombinant protein. Cells were harvested by centrifugation, resuspended in 20 mM Tris-HCl buffer (pH 7.4), and lysed by ultrasonication. The recombinant protein was purified using a His-tag Protein Purification Kit (Beyotime Biotechnology Co., Ltd., Shanghai, China) with a linear imidazole gradient (20-250 mM). Protein purity was analyzed by 12% SDS-PAGE, and the eluted protein was concentrated via ultrafiltration. Protein concentration was determined using a Bradford Protein Assay Kit (Beyotime Biotechnology Co., Ltd., Shanghai, China).

### 3.4. Biochemical Characterization of MhAly6

The alginate lyase activity of MhAly6 was measured using the DNS method [53]. Briefly, 900  $\mu$ L of 1 mg/mL sodium alginate was mixed with 100  $\mu$ L of the diluted enzyme solution and incubated at 40°C for 10 min. The reaction was terminated by adding 1.0 mL DNS, followed by boiling at 100°C for 5 min to develop color. After cooling to room temperature, the solution was diluted to a final volume of 5.0 mL, and the absorbance was measured at 540 nm. Heat-inactivated enzyme was used as the control. One unit (U) of the enzyme activity was defined as the amount of enzyme required to release 1  $\mu$ g of reducing sugar (glucose equivalent) per min.

The optimal temperature for MhAly6 activity was determined by measuring enzyme activity at various temperatures ranging from 25°C to 65°C in pH 8.0 buffer. Reactions were terminated by boiling after 20 min of incubation. Thermal stability was evaluated by pre-incubating the enzyme at 40°C, 45°C, or 50°C for varying durations. The optimal pH was determined using buffers with pH values ranging from 3.0 to 10.0 (citrate buffer for pH 3.0-6.0, phosphate buffer for pH 6.0-8.0, and glycine buffer for pH 8.0-10.0). The effect of NaCl on enzyme activity was evaluated by measuring activity in the presence of 0-1.0 M NaCl. Substrate specificity was determined using sodium alginate, Poly M and Poly G as substrates. The influence of metal ions and chemical reagents on MhAly6 was investigated by adding them to the reaction mixture at final concentrations of 1, 5, or 10 mM (for ions) or 0.1%, 0.5%, and 1% (for reagents).

### 3.5. Analysis of Degradation Products

The purified enzyme was mixed separately with three substrates-sodium alginate, Poly M, and Poly G-at a 1:9 ratio and allowed to react under optimal conditions for 0.5-24 h. To terminate the reactions, samples were boiled in a water bath for 10 min. The resulting products were purified via ethanol precipitation. After purification, an appropriate amount of the oligosaccharide powder was dissolved in deionized water and subsequently filtered through a sterile membrane (0.22  $\mu$ m). The product distribution at different degradation times was initially analyzed by TLC. To further characterize the products, negative-ion ESI-MS (Thermo Fisher Scientific Q Exactive Focus, USA) was employed to determine the distribution and DP of the products obtained after 24 h of degradation using sodium alginate as the substrate.

### 3.6. Structural Modeling and Molecular Docking of MhAly6

The three-dimensional structure of MhAly6 was predicted using both the SWISS-MODEL server and AlphaFold 3. The resulting models were evaluated using the SAVES v6.0 server. Molecular docking of MhAly6 with AOS (DP 6) was performed using AutoDock-Vina. The ligand poly M (M6, CID: 71761996) was downloaded from PubChem (<https://pubchem.ncbi.nlm.nih.gov/>). Poly G (G6) and poly MG (H6, a hexasaccharide formed by alternating  $\beta$ -1,4-glycosidic bonds between mannuronic and guluronic acids) were generated using ChemDraw. Format conversions were carried out using Open Babel. The docking mode with the lowest binding energy was selected for further analysis. Conservation analysis was performed using Consurf, and the docking results were visualized using PyMOL.

### 3.7. Antioxidant Properties of the Alginate Degradation Products Produced by MhAly6

#### 3.7.1. Ferric Reducing Capacity

The ferric reducing capacity of the alginate degradation products was determined according to a previously described method with minor modifications [54]. Briefly, 50  $\mu$ L of degradation product solutions with different concentrations were added to a 96-well plate, followed by sequential addition of 50  $\mu$ L sodium phosphate buffer (pH 6.6, 20 mM) and 50  $\mu$ L of potassium ferricyanide solution (1% w/v). After incubation at 50°C for 20 min, 50  $\mu$ L of (10% w/v) trichloroacetic acid containing (1% w/v)



ferric chloride was added to the reaction mixture and kept at room temperature for 10 min. The absorbance of the mixture was measured at 690 nm.

### 3.7.2. Hydroxyl Radical Scavenging Capacity

The hydroxyl radical scavenging capacity of the degradation products was determined using a modified salicylic acid method [55]. Briefly, 50  $\mu$ L of the degradation product solutions at varying concentrations, 50  $\mu$ L of FeSO<sub>4</sub> solution (9 mM), 50  $\mu$ L of salicylic acid-ethanol solution (9 mM), and 50  $\mu$ L of H<sub>2</sub>O<sub>2</sub> (8.8 mM) were sequentially added to a 96-well plate. After thorough mixing, the mixture was incubated in a 37°C water bath for 30 min, and the absorbance at 510 nm was recorded as A. A blank control (absorbance B) was prepared by replacing H<sub>2</sub>O<sub>2</sub> with deionized water, and a negative control (absorbance C) was prepared by replacing the degradation product solution with deionized water. Vc at the same concentrations was used as a positive control. The hydroxyl radical scavenging rate was calculated using the formula (1):

$$\text{Scavenging effect (\%)} = (B - A)/(B - C) \times 100 \quad (1)$$

### 3.7.3. Scavenging Activity of 2,2-Diphenyl-1-picrylhydrazyl (DPPH)

Under dark conditions, different mass concentrations of degradation product solutions and an equal volume of DPPH solution (0.2 mM) were sequentially added to a 96-well plate. After incubation at 25°C for 30 min, the absorbance at 517 nm was measured and recorded as A [56]. A blank control (absorbance B) was prepared by replacing the DPPH solution with absolute ethanol, and a negative control (absorbance C) was prepared by replacing the degradation product solution with deionized water. Vc at the same concentrations was used as a positive control. The DPPH radical scavenging rate was calculated using the formula (1).

### 3.7.4. Scavenging Activity of 2,2'-Azinobis-(3-ethylbenzthiazoline-6-sulphonate) (ABTS)

The ABTS free radical scavenging activity was determined using a modified version of a previously described method [57]. The stock solution of ABTS radical was prepared by mixing ABTS (7 mM) and K<sub>2</sub>S<sub>2</sub>O<sub>8</sub> (88 mM) solutions at a volume ratio of 5:88, followed by storage in the dark for 16 h to generate ABTS free radicals. The stock solution was diluted with absolute ethanol to achieve an absorbance of  $1.4 \pm 0.05$  at 405 nm, yielding the ABTS radical working solution. Equal volumes of the ABTS radical working solution and degradation product solutions at varying concentrations were mixed and incubated at 25°C for 30 min. The absorbance at 405 nm was recorded as A. A blank control (absorbance B) was prepared by replacing the ABTS radical working solution with absolute ethanol, and a negative control (absorbance C) was prepared by replacing the degradation product solution with deionized water. Vc at the same concentrations was used as a positive control. The ABTS radical scavenging rate was calculated using the formula (1).

## 4. Conclusions

To date, no alginate lyases from the genus 335 have been characterized. This study represents the first report on the biochemical properties of an alginate lyase from this genus, providing critical insights for understanding and utilizing the biotechnological potential of the *Mesonía* species. In this paper, we described the cloning and characterization of a novel PL6 family alginate lyase, MhAly6, from *Mesonía hitae* R32. The MhAly6 exhibited optimal activity at 45°C and pH 9.0, along with exceptional thermal stability at 40°C, retaining over 50% activity after 210 min of incubation. The enzyme showed tolerance to multiple metal ions at 1 mM and displayed Na<sup>+</sup>-dependent activation. MhAly6 efficiently degraded sodium alginate, poly M, and poly G, with the highest activity towards its natural substrate sodium alginate. The degradation products were AOS with DP ranging from 2 to 7. Antioxidant assays revealed that MhAly6-derived AOS displayed significant radical-scavenging activity, emphasizing their potential for applications in antioxidant-based products.

**Author Contributions:** Methodology, formal analysis, Y.S.Y. and Z.Y.L.; writing—original draft, and data curation, Y.S.Y., Y.Z. and D.F.Y.; Conceptualization, supervision, and funding acquisition, Y.Z. and X.J.G. All authors have read and agreed to the published version of the manuscript.

**Funding:** The research is kindly funded by the National Natural Science Foundation of China (Grant No. 31900088).

**Institutional Review Board Statement:** Not applicable.

**Data Availability Statement:** The data in this study are contained within the article; further inquiries can be directed to the corresponding author.

**Acknowledgments:** The research is kindly funded by the National Natural Science Foundation of China (Grant No. 31900088). The authors extend their gratitude to Ms. Li Yingchun from Shiyanjia Lab (www.shiyanjia.com) for providing invaluable assistance with the ESI-MS analysis.

**Conflicts of Interest:** The authors declare that they have no known competing financial interests or personal relationships that could have appeared to influence the work reported in this paper.

## Abbreviations

M	$\beta$ -D-mannuronic acid
G	$\alpha$ -L-guluronic acid
Mw	Molecular weight
Poly M	Poly $\beta$ -D-mannuronic acid
Poly G	Poly $\alpha$ -L-guluronic acid
AOS	Alginate oligosaccharides
DP	Degrees of polymerization
PL	Polysaccharide lyase
IPTG	Isopro-pyl- $\beta$ -D-thiogalactopyranoside
TLC	Thin-layer chromatography
ESI-MS	Electrospray ionization mass spectrometry
Vc	Ascorbic acid
DPPH	2,2-Diphenyl-1-picrylhydrazyl
ABTS	2,2'-Azinobis-(3-ethylbenzthiazoline-6-sulphonate)

## References

1. Grobler, C.E.; Mabate, B.; Prins, A.; Le Roes-Hill, M.; Pletschke, B.I. Expression, Purification, and Characterisation of Recombinant Alginate Lyase (*Flammeovirga* AL2) for the Bioconversion of Alginate into Alginate Oligosaccharides. *Molecules* **2024**, *29*, 5578.
2. Pirouzzadeh, M.; Moraffah, F.; Samadi, N.; Sharifzadeh, M.; Motasadizadeh, H.; Vatanara, A. Enhancement of Burn Wound Healing Using Optimized Bioactive Probiotic-Loaded Alginate Films. *Int. J. Biol. Macromol.* **2025**, *301*, 140454.
3. Alkhayer, M.; Hamzehpour, N.; Eghbal, M.K.; Rahnemaie, R. The Use of Magnesium-Enriched Brine for Stabilization of Highly Erodible Playa Surfaces: A Comparative Study with Sodium Alginate and Sodium Silicate. *J. Environ. Manage.* **2024**, *371*, 123339.
4. Queiroz, L.P. de O.; Aroucha, E.M.M.; dos Santos, F.K.G.; Souza, R.L. da S. e; Nunes, R.I.; Leite, R.H. de L. Influence of Alginate Extraction Conditions from the Brown Seaweed *Dictyota Mertensii* on the Functional Properties of a Novel Glycerol Plasticized Alginate Film. *Carbohydr. Polym.* **2025**, *352*, 123225.
5. Feng, Q.; Luo, Y.; Liang, M.; Cao, Y.; Wang, L.; Liu, C.; Zhang, X.; Ren, L.; Wang, Y.; Wang, D.; et al. Rhizobacteria Protective Hydrogel to Promote Plant Growth and Adaptation to Acidic Soil. *Nat. Commun.* **2025**, *16*, 1684.
6. Gu, X.; Fu, L.; Wang, Z.; Cao, Z.; Zhao, L.; Seswita-Zilda, D.; Zhang, A.; Zhang, Q.; Li, J. A Novel Bifunctional Alginate Lyase and Antioxidant Activity of the Enzymatic Hydrolysates. *J. Agric. Food Chem.* **2024**, *72*, 4116–4126.
7. Qiu, X.-M.; Lin, Q.; Zheng, B.-D.; Zhao, W.-L.; Ye, J.; Xiao, M.-T. Preparation and Potential Antitumor Activity of Alginate Oligosaccharides Degraded by Alginate Lyase from *Cobetia Marina*. *Carbohydr. Res.* **2023**, *534*, 108962.

8. Ribeiro, D.M.; Luise, D.; Costa, M.; Carvalho, D.F.P.; Martins, C.F.; Correa, F.; Pinho, M.; Mirzapour-Kouhdasht, A.; Garcia-Vaquero, M.; Mourato, M.P.; et al. Impact of Dietary *Laminaria Digitata* with Alginate Lyase or Carbohydrase Mixture on Nutrient Digestibility and Gut Health of Weaned Piglets. *Animal* **2024**, *18*, 101189.
9. Ribeiro, D.M.; Leclercq, C.C.; Charton, S.A.B.; Costa, M.M.; Carvalho, D.F.P.; Cocco, E.; Sergeant, K.; Renaut, J.; Freire, J.P.B.; Prates, J.A.M.; et al. Enhanced Ileum Function in Weaned Piglets via *Laminaria Digitata* and Alginate Lyase Dietary Inclusion: A Combined Proteomics and Metabolomics Analysis. *J. Proteomics* **2023**, *289*, 105013.
10. Oulad Ziane, S.; Imehli, Z.; El Alaoui Talibi, Z.; Ibsouda Koraichi, S.; Meddich, A.; El Modafar, C. Biocontrol of Tomato Verticillium Wilt Disease by Plant Growth-Promoting Bacteria Encapsulated in Alginate Extracted from Brown Seaweed. *Int. J. Biol. Macromol.* **2024**, *276*, 133800.
11. Zhu, B.; Li, L.; Yuan, X. Efficient Preparation of Alginate Oligosaccharides by Using Alginate Lyases and Evaluation of the Development Promoting Effects on *Brassica Napus* L. in Saline-Alkali Environment. *Int. J. Biol. Macromol.* **2024**, *270*, 131917.
12. Teng, Y.; Li, J.; Guo, J.; Yan, C.; Wang, A.; Xia, X. Alginate Oligosaccharide Improves 5-Fluorouracil-Induced Intestinal Mucositis by Enhancing Intestinal Barrier and Modulating Intestinal Levels of Butyrate and Isovalerate. *Int. J. Biol. Macromol.* **2024**, *276*, 133699.
13. Abdo, A.A.A.; Hou, Y.; Hassan, F.A.; Al-Sheraji, S.H.; Aleryani, H.; Alanazi, A.; Sang, Y. Antioxidant Potential and Protective Effect of Modified Sea Cucumber Peptides against H<sub>2</sub>O<sub>2</sub>-Induced Oxidative Damage in Vitro HepG2 Cells and in Vivo Zebrafish Model. *Int. J. Biol. Macromol.* **2024**, *266*, 131090.
14. Singh, S.; Uddin, M.; Singh, S.; Ahmed, K.B.M.; Bhat, U.H.; Chishti, A.S.; Chauhan, A.; Khan, M.M.A. Radiolytically Depolymerized Low Molecular-Weight Chitosan (ICH) and Sodium Alginate (ISA) Improve Growth Attributes, Physiological Performance and the Production of Steviol Glycosides (SGs) of *S. Rebaudiana* (Bertoni). *J. Polym. Environ.* **2024**, *32*, 3258–3284.
15. Samdurkar, A.N.; Choudhary, A.D.; Varshney, L.; Badere, R.S. Application of 28.1 kDa Alginate Oligosaccharide Improves the Yield and Quality of Grain in Rice. *ChemistrySelect* **2024**, *9*, e202400742.
16. Aly, A.A.; Eliwa, N.E.; Safwat, G. Role of Gamma-Irradiated Sodium Alginate on Growth, Physiological and Active Components of Iceberg Lettuce (*Lactuca Sativa*) Plant. *BMC Plant Biol.* **2024**, *24*, 185.
17. Song, Y.H.; Woo, H.C.; Lee, J. Eco-Friendly Depolymerization of Alginates by H<sub>2</sub>O<sub>2</sub> and High-Frequency Ultrasonication. *Clean Technologies* **2023**, *5*, 1402–1414.
18. Ye, Y.; Zhang, Y.; Zhou, Y.; Gao, Y. Molecular Engineering of Alginate Lyases and the Potential Agricultural Applications of Their Enzymatic Products. *J. Agric. Food Chem.* **2025**, Published online February 26.
19. Lu, S.; Na, K.; Wei, J.; Zhang, L.; Guo, X. Alginate Oligosaccharides: The Structure-Function Relationships and the Directional Preparation for Application. *Carbohydr. Polym.* **2022**, *284*, 119225.
20. Zhou, J.; Li, J.; Chen, G.; Zheng, L.; Mei, X.; Xue, C.; Chang, Y. Discovery and Characterization of a Novel Poly-Mannuronate Preferred Alginate Lyase: The First Member of a New Polysaccharide Lyase Family. *Carbohydr. Polym.* **2024**, *343*, 122474.
21. Xu, C.; Xiong, Y.; Wang, Q.; Fang, F.; Wang, J.; Huang, S.; Xu, J.; Peng, Y.; Xie, C. Isolation of Salt-Tolerant *Vibrio Alginolyticus* X511 for Efficient Co-Production of 2,3-Butanediol and Alginate Lyase from *Laminaria Japonica*. *Int. J. Biol. Macromol.* **2025**, *288*, 138765.
22. Peng, C.; Wang, Q.; Xu, W.; Wang, X.; Zheng, Q.; Liang, X.; Dong, X.; Li, F.; Peng, L. A Bifunctional Endolytic Alginate Lyase with Two Different Lyase Catalytic Domains from *Vibrio* Sp. H204. *Front. Microbiol.* **2024**, *15*, 1509599.
23. Li, X.; Yang, M.; Mo, K.; Hu, Y.; Gu, H.; Sun, D.; Bao, S.; Huang, H. Genome Analysis of Multiple Polysaccharide-Degrading Bacterium *Microbulbifer Thermotolerans* HB226069: Determination of Alginate Lyase Activity. *Mar. Biotechnol.* **2024**, *26*, 488–499.
24. Nishiyama, R.; Ojima, T.; Ohnishi, Y.; Kumaki, Y.; Aizawa, T.; Inoue, A. An Oxidative Metabolic Pathway of 4-Deoxy-L-Erythro-5-Hexoseulose Uronic Acid (DEHU) from Alginate in an Alginate-Assimilating Bacterium. *Commun. Biol.* **2021**, *4*, 1254.
25. Nguyen, T.N.T.; Chataway, T.; Araujo, R.; Puri, M.; Franco, C.M.M. Purification and Characterization of a Novel Alginate Lyase from a Marine *Streptomyces* Species Isolated from Seaweed. *Mar. Drugs* **2021**, *19*, 590.
26. Zeng, L.; Li, J.; Gu, J.; Hu, W.; Han, W.; Li, Y. Alginate-Degrading Modes, Oligosaccharide-Yielding Properties, and Potential Applications of a Novel Bacterial Multifunctional Enzyme, Aly16-1. *Microorganisms* **2024**, *12*, 2374.
27. Nedashkovskaya, O.I. *Mesonina Algae Gen. Nov., Sp. Nov.*, a Novel Marine Bacterium of the Family Flavobacteriaceae Isolated from the Green Alga *Acrosiphonia Sonderi* (Kütz.) Kornm. *Int. J. Syst. Evol. Microbiol.* **2003**, *53*, 1967–1971.
28. Na Wang; Jia Rong Liu; Xi Ying Zhang; Shen Fan; Yu Zhong Zhang; Hui Hui Fu *Mesonina Profundi* Sp. Nov., Isolated from Deep-Sea Sediment of the Mariana Trench. *Int. J. Syst. Evol. Microbiol.* **2024**, *74*.
29. Rao, H.; Huan, R.; Chen, Y.; Xiao, X.; Li, W.; He, H. Characteristics and Application of a Novel Cold-Adapted and Salt-Tolerant Protease EK4-1 Produced by an Arctic Bacterium *Mesonina Algae* K4-1. *Int. J. Mol. Sci.* **2023**, *24*, 7985.

30. Zhou, Y.; Gao, X.; Xu, J.; Li, G.; Ma, R.; Yan, P.; Dong, C.; Shao, Z. *Mesonina Hitae* Sp. Nov., Isolated from the Seawater of the South Atlantic Ocean. *Int. J. Syst. Evol. Microbiol.* **2021**, *71*.
31. Wang, X.; Hu, R.; Zhang, Y.; Tian, L.; Liu, S.; Huang, Z.; Wang, L.; Lu, Y.; Wang, Y.; et al. Mechanistic Analysis of Thermal Stability in a Novel Thermophilic Polygalacturonase MIPG28B Derived from the Marine Fungus *Mucor Lusitanicus*. *Int. J. Biol. Macromol.* **2024**, *280*, 136007.
32. Mathieu, S.; Henrissat, B.; Labre, F.; Skjåk-Bræk, G.; Helbert, W. Functional Exploration of the Polysaccharide Lyase Family PL6. *PLoS ONE* **2016**, *11*, e0159415.
33. Wang, B.; Dong, S.; Li, F.-L.; Ma, X.-Q. Structural Basis for the Exolytic Activity of Polysaccharide Lyase Family 6 Alginate Lyase BcAlyPL6 from Human Gut Microbe *Bacteroides Clarus*. *Biochem. Biophys. Res. Commun.* **2021**, *547*, 111–117.
34. Guo, Q.; Dan, M.; Zheng, Y.; Shen, J.; Zhao, G.; Wang, D. Improving the Thermostability of a Novel PL-6 Family Alginate Lyase by Rational Design Engineering for Industrial Preparation of Alginate Oligosaccharides. *Int. J. Biol. Macromol.* **2023**, *249*, 125998.
35. Xu, F.; Dong, F.; Wang, P.; Cao, H.-Y.; Li, C.-Y.; Li, P.-Y.; Pang, X.-H.; Zhang, Y.-Z.; Chen, X.-L. Novel Molecular Insights into the Catalytic Mechanism of Marine Bacterial Alginate Lyase AlyGC from Polysaccharide Lyase Family 6\*. *J. Biol. Chem.* **2017**, *292*, 4457–4468.
36. Wu, M.; Cao, L.; Tang, W.; Liu, Z.; Feng, S. Improving the Anti-Autolytic Ability of Alkaline Protease from *Bacillus Alcalophilus* by a Rationally Combined Strategy. *Enzyme Microb. Technol.* **2025**, *184*, 110561.
37. Watanabe, K.; Masuda, T.; Ohashi, H.; Mihara, H.; Suzuki, Y. Multiple Proline Substitutions Cumulatively Thermostabilize *Bacillus Cereus* ATCC7064 Oligo-1,6-Glucosidase. *Eur. J. Biochem.* **1994**, *226*, 277–283.
38. Gao, S.; Zhang, Z.; Li, S.; Su, H.; Tang, L.; Tan, Y.; Yu, W.; Han, F. Characterization of a New Endo-Type Polysaccharide Lyase (PL) Family 6 Alginate Lyase with Cold-Adapted and Metal Ions-Resisted Property. *Int. J. Biol. Macromol.* **2018**, *120*, 729–735.
39. Belik, A.; Silchenko, A.; Malyarenko, O.; Rasin, A.; Kiseleva, M.; Kusaykin, M.; Ermakova, S. Two New Alginate Lyases of PL7 and PL6 Families from Polysaccharide-Degrading Bacterium *Formosa Algae* KMM 3553<sup>T</sup>: Structure, Properties, and Products Analysis. *Mar. Drugs* **2020**, *18*, 130.
40. Li, Q.; Hu, F.; Wang, M.; Zhu, B.; Ni, F.; Yao, Z. Elucidation of Degradation Pattern and Immobilization of a Novel Alginate Lyase for Preparation of Alginate Oligosaccharides. *Int. J. Biol. Macromol.* **2020**, *146*, 579–587.
41. Cheng, D.; Liu, Z.; Jiang, C.; Li, L.; Xue, C.; Mao, X. Biochemical Characterization and Degradation Pattern Analysis of a Novel PL-6 Alginate Lyase from *Streptomyces Coelicolor* A3(2). *Food Chem.* **2020**, *323*, 126852.
42. Xue, Z.; Sun, X.-M.; Chen, C.; Zhang, X.-Y.; Chen, X.-L.; Zhang, Y.-Z.; Fan, S.-J.; Xu, F. A Novel Alginate Lyase: Identification, Characterization, and Potential Application in Alginate Trisaccharide Preparation. *Mar. Drugs* **2022**, *20*, 159.
43. Long, L.; Hu, Q.; Wang, X.; Li, H.; Li, Z.; Jiang, Z.; Ni, H.; Li, Q.; Zhu, Y. A Bifunctional Exolytic Alginate Lyase from *Microbulbifer* Sp. ALW1 with Salt Activation and Calcium-Dependent Catalysis. *Enzyme Microb. Technol.* **2022**, *161*, 110109.
44. He, X.; Zhang, Y.; Wang, X.; Zhu, X.; Chen, L.; Liu, W.; Lyu, Q.; Ran, L.; Cheng, H.; Zhang, X.-H. Characterization of Multiple Alginate Lyases in a Highly Efficient Alginate-Degrading *Vibrio* Strain and Its Degradation Strategy. *Appl. Environ. Microbiol.* **2022**, *88*, e01389-22.
45. Zheng, Y.; Wang, Y.; Dan, M.; Li, Y.; Zhao, G.; Wang, D. Characterization of Degradation Patterns and Enzymatic Properties of a Novel Alkali-Resistant Alginate Lyase AlyRm1 from *Rubrivirga Marina*. *Curr. Res. Food Sci.* **2023**, *6*, 100414.
46. Cao, S.; Li, L.; Zhu, B.; Yao, Z. Elucidation of Non-Catalytic Domain Alterations Effects on Properties and Action Pattern of a Novel Alginate Lyase. *Process Biochem.* **2023**, *133*, 39–48.
47. Waterhouse, A.; Bertoni, M.; Bienert, S.; Studer, G.; Tauriello, G.; Gumienny, R.; Heer, F.T.; deBeer, T.A.P.; Rempfer, C.; Bordoli, L.; et al. SWISS-MODEL: Homology Modelling of Protein Structures and Complexes. *Nucleic Acids Res.* **2018**, *46*, W296–W303.
48. Studer, G.; Rempfer, C.; Waterhouse, A.M.; Gumienny, R.; Haas, J.; Schwede, T. QMEANDisCo-Distance Constraints Applied on Model Quality Estimation. *Bioinformatics* **2020**, *36*, 1765–1771.
49. Abramson, J.; Adler, J.; Dunger, J.; Evans, R.; Green, T.; Pritzel, A.; Ronneberger, O.; Willmore, L.; Ballard, A.J.; Bambrick, J.; et al. Accurate Structure Prediction of Biomolecular Interactions with AlphaFold 3. *Nature* **2024**, *630*, 493–500.
50. Pontius, J.; Richelle, J.; Wodak, S.J. Deviations from Standard Atomic Volumes as a Quality Measure for Protein Crystal Structures. *J. Mol. Biol.* **1996**, *264*, 121–136.
51. Zhang, Y.-H.; Shao, Y.; Jiao, C.; Yang, Q.-M.; Weng, H.-F.; Xiao, A.-F. Characterization and Application of an Alginate Lyase, Aly1281 from Marine Bacterium *Pseudoalteromonas Carrageenovora* ASY5. *Mar. Drugs* **2020**, *18*, 95.
52. Kelishomi, Z.H.; Goliaei, B.; Mahdavi, H.; Nikoofar, A.; Rahimi, M.; Moosavi-Movahedi, A.A.; Mamashli, F.; Bigdeli, B. Antioxidant Activity of Low Molecular Weight Alginate Produced by Thermal Treatment. *Food Chem.* **2016**, *196*, 897–902.



53. Miller, G.L. Use of Dinitrosalicylic Acid Reagent for Determination of Reducing Sugar. *Anal. Chem.* **1959**, *31*, 426–428.
54. Chang, C.-Y.; Wu, K.-C.; Chiang, S.-H. Antioxidant Properties and Protein Compositions of Porcine Haemoglobin Hydrolysates. *Food Chem.* **2007**, *100*, 1537–1543.
55. Yang, J.; Cui, D.; Ma, S.; Chen, W.; Chen, D.; Shen, H. Characterization of a Novel PL 17 Family Alginate Lyase with Exolytic and Endolytic Cleavage Activity from Marine Bacterium *Microbulbifer* Sp. SH-1. *Int. J. Biol. Macromol.* **2021**, *169*, 551–563.
56. Alashi, A.M.; Blanchard, C.L.; Mailer, R.J.; Agboola, S.O.; Mawson, A.J.; He, R.; Girgih, A.; Aluko, R.E. Antioxidant Properties of Australian Canola Meal Protein Hydrolysates. *Food Chem.* **2014**, *146*, 500–506.
57. Puja, B.K.; Mallick, S.; Dey, T.; Chanda, S.; Ghosh, S. Xylooligosaccharide Recovery from Sugarcane Bagasse Using  $\beta$ -Xylosidase-Less Xylanase, BsXln1, Produced by *Bacillus Stercoris* DWS1: Characterization, Antioxidant Potential and Influence on Probiotics Growth under Anaerobic Conditions. *Int. J. Biol. Macromol.* **2025**, *285*, 138307.

**Disclaimer/Publisher's Note:** The statements, opinions and data contained in all publications are solely those of the individual author(s) and contributor(s) and not of MDPI and/or the editor(s). MDPI and/or the editor(s) disclaim responsibility for any injury to people or property resulting from any ideas, methods, instructions or products referred to in the content.